Arachidonic Acid Blocks Large-Conductance Chloride Channels in L6 Myoblasts

J. ZACHAR and O. HURŇÁK

Institute of Molecular Physiology and Genetics, Slovak Academy of Sciences, Vlárska 5, 833 34 Bratislava, Slovak Republic

Abstract. Modulation of high-conductance chloride channels by eicosanoids, stilbene derivatives and Zn^{2+} ions was studied in cultured myoblasts (L6 rat muscle cell line) in excised and cell-attached membrane patches using a conventional patch clamp method.

Arachidonic acid (AA) blocked the channel at concentrations 1 – 50 μmol/l from the internal side of the membrane in excised (inside out) patches with a time constant of about 20 s. The block was absent when arachidonic acid was applied to the bathing solution in cell attached patches, or to the pipette solution, respectively.

Arachidonic acid changed the probability of the channel being in the open state (P_{open}) in dependence on the applied voltage (V). The asymmetric bell-shaped $P_{open} - V$ relationship showed a steeper dependence on both the negative and positive voltage, respectively, in arachidonic acid solutions. The midpoint potentials (V_h) of the P_{open} – V relationship were shifted towards lower membrane potential displacements from the holding potential.

The recovery from the block was very slow but was found to be enhanced by application of a symmetric voltage ramp pulse.

The stilbene derivative (DIDS) blocked the channel at μmolar concentrations (10–100 μmol/l) applied from the internal side of the membrane. The onset and recovery of the DIDS block showed characteristics similar to the AA block.

The channel was found to be blocked reversibly by short application of Zn^{+} ions (1–10 mmol/l) from the internal side of the membrane.

Key words: Chloride channel — Large conductance channel — Maxi-Cl channel — Anion channel — Muscle cell line — L6 myoblasts — Stilbene derivatives — DIDS — Zn ions — Arachidonic acid — Patch clamp

Dedicated to memory of Daria Zacharová MD, PhD (1924–1994)

Introduction

The-large conductance chloride channels are blocked by several drugs and agents. Most blockators are, however, non-specific, as they are known to affect also other channels and/or membrane transport systems (i.e. stilbene derivatives or Zn^{2+}). Few physiological modulators of large-conductance chloride channels have been so far suggested, i.e. substances which were natural products of physiological processes (Kemp et al. 1993; Bettendorf et al. 1993). Such substances, if verified and/or discovered, would narrow the possibilities so far suggested for the functional significance of the maxi-Cl channels.

With this aim in mind we tested the effects of arachidonic acid, which makes up a major component of membrane phospholipids (Irvine 1982), on the maxi-Cl channel activity in L6 myoblasts. Arachidonic acid is known to stimulate or inhibit directly and indirectly a number of channel types in a variety of cells (for a review see Ordway et al. 1991). Although the evidence concerns mostly the exogenously applied arachidonic acid, there is also evidence that arachidonic acid liberated by agonist stimulation, and the active metabolites that are generated subsequently (Axelrod 1990), participate in the regulation of ion channels (Piomelli et al. 1987; Kurachi et al. 1989).

In this paper we describe at first the effects of arachidonic acid, which turned out to be a potent blockator of maxi-Cl channels from the internal side of the membrane, and then the effects of two common blockators of maxi-Cl channels, the stilbene derivatives and the Zn^{2+} ions.

Materials and Methods

Solutions. The standard bath contained a Krebs solution consisting of (mmol/l): 135 NaCl; 5 KCl; 1 $CaCl_2$; 1 $MgCl_2$; 20 HEPES; 5 glucose; pH 7.4 at 23 °C or physiological solution: 150 NaCl; 0.5 $CaCl_2$; 20 HEPES; pH 7.4. In most experiments the pipette solution was the same as that in the bath solution. The blocking agents were added to the standard bath saline at indicated concentrations. All experiments in the inside-out patch configuration that required exchange of solutions were performed with the tip of the patch pipette positioned inside a perfusion capillary with a diameter of about 1 mm. Introduction of the patch pipette into the capillary by means of two micromanipulators (for perfusion pipette and patch pipette respectively) was followed on the screen of a TV monitor connected to a microscope video system. This procedure allowed close control of the solution bathing the intracellular surface of the excised membrane and safe exchange of solution without mechanical disturbances and release of the seal. This was a threat in cell-attached patches, when the whole bath solution was being exchanged. The perfusion pipette was situated close to a three-way tap; the dead time of exchange was about 10 s. Arachidonic acid (AA) was initially dissolved in 100% ethanol, and all experimental dilutions were at a final ethanol concentration of 0.1% (vol/vol). Ethanol (0.1%) alone did not alter basic characteristics of the channel unit activity. The stilbene derivative, DIDS (4,4′-diisothiocyanatostilbene-2,2′-disulphonic acid) was purchased from Sigma (St.

Louis, MO, USA). Zn^{2+} solutions were used with Cl^- anion and required slight pH adjustment.

Cells. The stable rat muscle cell line L6 was used for patch clamp experiments. The procedures of culture maintenance and manipulation before and during experiments are described elsewhere (Hurňák and Zachar 1994). The measurements were mostly made on rounded-up proliferating myoballs.

Electrophysiology. Currents were recorded in cell-attached or excised (inside-out) configuration of the patch-clamp technique (Hamill et al. 1981) as described in detail elsewhere (Hurňák and Zachar 1992) and shortly by Hurňák and Zachar (1994). Voltage-dependence of channel activation was determined as described in detail elsewhere (Hurňák and Zachar 1993). Fitting of the $P_{open} - V$ relationship and drawing of three dimensional graphs from the records was performed by means of protocols written in Mathematica 2.1 software (Wolfram Research, Champaign, IL, USA). Voltages represent pipette potentials.

Results

The effect of arachidonic acid

Fig. 1 demonstrates the inhibitory effect of 25 μmol/l arachidonic acid (AA) on the unit current records in L6 myoblasts (right-hand column; panels *C*, *D*). The patch membrane contained several (at least 5) maxi-Cl channels activated by repeated ± 20 mV pulses (≈ 5 s in duration) in Krebs solution (left-hand column; panels *A* and *B*). Fig. 1*A* demonstrates 5 unit current records to positive pulses and Fig. 1*B* the same number of records to negative pulses, respectively, from the holding potential, $HP = 0$ mV in symmetrical chloride solutions ([Cl] = 147 mmol/l; Krebs saline). The unit channel activity was considerably depressed after introduction of the AA solution (25 μmol/l) to the excised (inside-out) patch membrane. Five records in Fig. 1*C* and Fig. 1*D* are from a long series of recordings starting at about 1.5 min after introduction of arachidonic acid to the *macropipette* bathing the patch pipette with the excised membrane.

The ensemble average currents from recordings demonstrated in Fig. $1A - D$ are shown in panels $1a - d$. It is evident that the responses (Fig. $1a, b$) to symmetrical positive and negative pulses in symmetrical Krebs solutions show typical asymmetry, as far as the inactivation of the summated chloride current is concerned. The ensemble Cl current to +20 mV pulses (a) did not inactivate at all and that to -20 mV pulses (b) inactivated with a time constant of 2.6 s. After about 1.5 min the ensemble Cl currents were considerably decreased. The inward Cl current (c) shows in addition inactivation, whilst the outward Cl current (d) was maintained at a plateau of about 15 pA. By inspection of the records (D) it could be easily recognised that the plateau is due to a delay in activation of the two channels which were not blocked.

The complete course of the AA block development (25 μmol/l) is shown by three dimensional graphs in Figs. 2*A* and 2*B*. The x axis gives the distribution

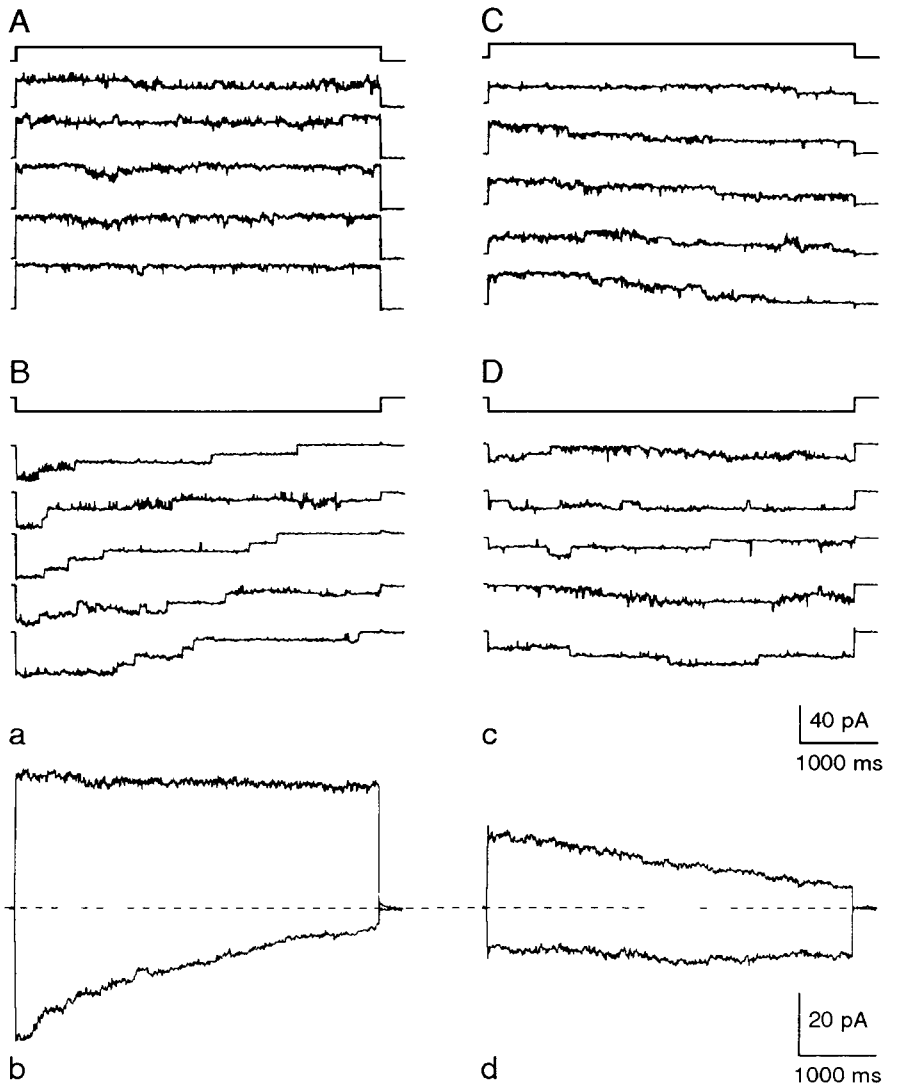

Figure 1. Single-channel currents recorded from an excised patch (inside-out) of a proliferating L6 myoblast in control Krebs solution (*A*, *B*, *a*, *b*) and 1.5 min after addition of arachidonic acid (25 μmol/l) to the Krebs solution (*C*, *D*, *c*, *d*) respectively. *A* – *D* Five consecutive single-channel current traces to repeated command potentials of ± 20 mV and 4750 ms in duration applied at 10 s intervals. The holding potential was 0 mV. *a* – *d* Ensemble averages of single-channel currents from the records shown in *A* – *D*.

of current amplitudes (pA) in response to successive negative (*A*, *a*) and positive (*B*, *b*) 20 mV pulses, respectively. The zeros of the *a* axis represent the closed

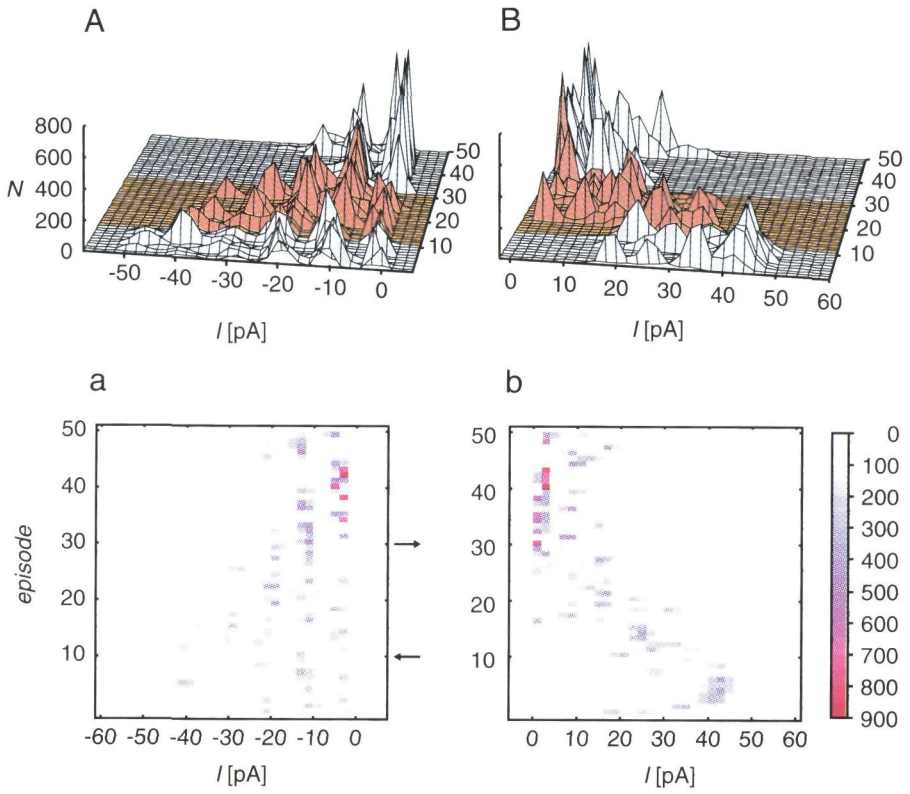

Figure 2. Three-dimensional ($A - B$) view of successive unit channel current records to repeated negative (A) and positive (B) 20 mV pulses during the development of arachidonic acid block in an excised patch membrane containing up to 5 maxi-Cl channels. x *axis*: distribution of unit channel currents in pA; y *axis*: sequence of successive episodes; z *axis*: number (N) of events at corresponding current amplitudes. Two-dimensional projections of A and B on the $x - y$ plane are shown in a and b. The height of current peaks (N) is represented by different colors (see color scale). Left arrows (←) indicate introduction and right arrows (→) withdrawal of arachidonic acid respectively from the bathing Krebs solution. Ice blue color: control Krebs solution; hot pink color: 25 μmol/l arachidonic acid Krebs solution.

state of the channel. The y axis gives the succession of responses to the applied pulses (episodes) and can be easily transformed into a time axis by multiplying the episodes with the repetition interval (as shown in Fig. 3). The z axis shows the number of events (N) at given current amplitudes. The change to a new bathing solution is denoted by a change of color of the crossed base plate of the 3D graph. Records in 25 μmol/l arachidonic acid solution are shown in hot pink color. Ice

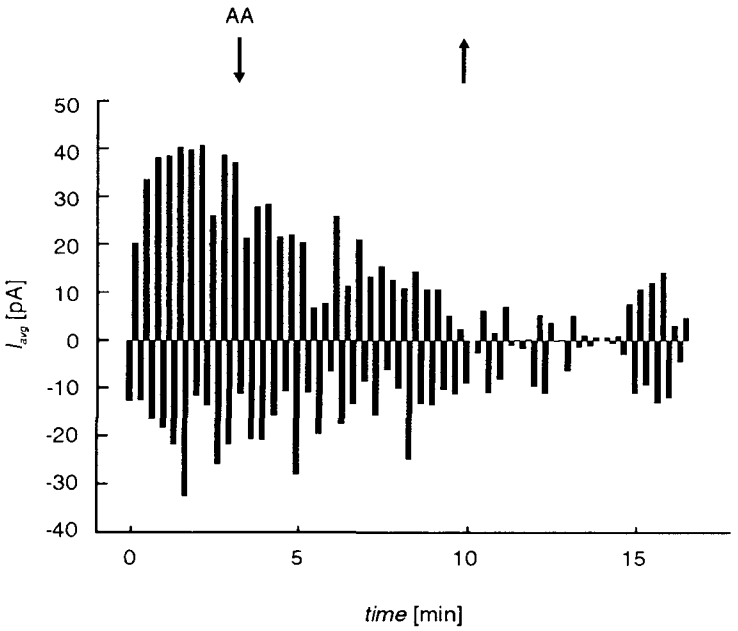

Figure 3. Bar chart presentation of the arachidonic acid block development. *Ordinate (pA)*: individual bars represent averaged amplitudes of the unit channel currents to single negative (downwards) and positive (upwards) 20 mV command pulses, respectively. *Abscissa*: time in min from the start of recording. Arrows indicate introduction (downwards) or withrawal (upwards) of arachidonic acid from the internal side of the membrane.

blue color denotes control Krebs solution. Figs. 2*a* and 2*b* are two-dimensional projections of the above three dimensional graphs to show the shift in distribution of the unit channel currents with time and/or successive records (episodes). The height of peaks (N) in A and B is represented in the $x - y$ projections by scaled colors. The development of the block by arachidonic acid manifests itself by the shift of channel currents towards lower and eventually up to zero values. The graphs also conclusively demonstrate (especially Figs. 2 *a* and *b*) that the block in arachidonic acid ensues with a delay of several tens of seconds, and that the block is not reversible. The time relations of the block development are best seen in Fig. 3. The bars represent summated currents in each episode to positive (upward) and negative (downward) pulses, respectively. The application and withdrawal of arachidonic acid (25 μmol/l) are denoted by arrows. As follows from the graph, the channel block developed with a relatively long time constant and did not reach the final blocked level before the exchange of AA solution for Krebs solution. The development of the block continued even in the recovery Krebs solution. The

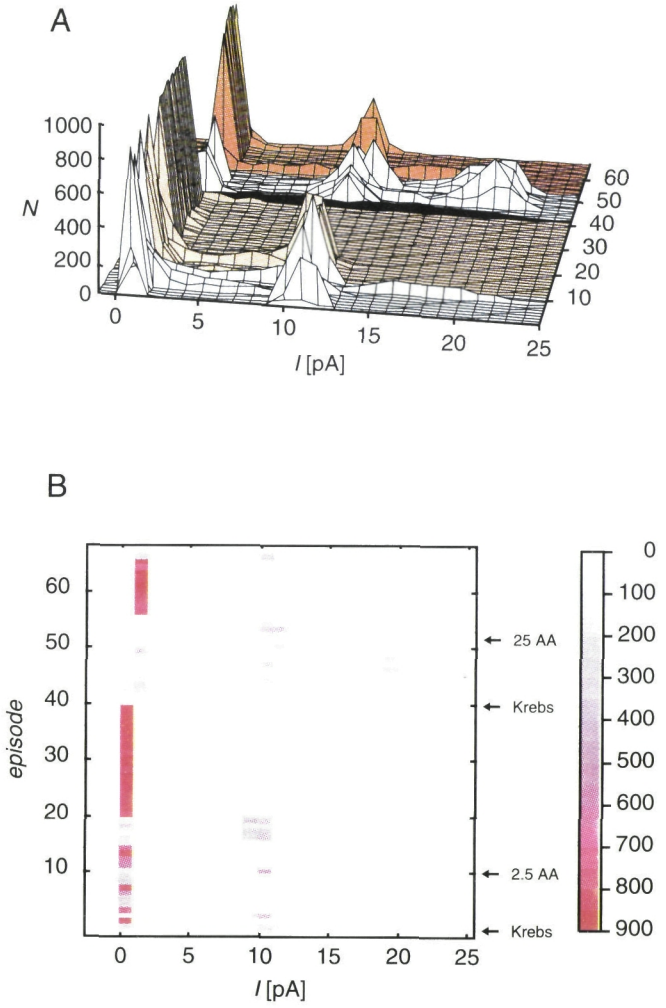

Figure 4. Development of arachidonic acid block in an excised patch membrane containing 1 maxi-Cl channel at the start of the experiment. Single channel currents to +20 mV pulses (4750 ms in duration applied at 10 s intervals). *A*. Three-dimensional graph with axes as described in Fig. 2. Ice blue color indicates records in Krebs solution, faded pink color indicates records in arachidonic acid (2.5 μmol/l) containing Krebs solution, hot pink color indicates records in 25 μmol/l arachidonic solution. Note activation of the second maxi-Cl channel during recovery after application of a ramp pulse (from −40 to +40 mV) preceeding the episode shown in black. Both channels were inhibited by the second application of AA (25 μmol/l). *B*. Two-dimensional projection of graph *A* on the $x - y$ plane. The height of current peaks (N) is represented by different colors (see color scale). Arrows (←) indicate introduction of tested solutions. AA – arachidonic acid Krebs solution; 2.5 and 25 μmol/l, respectively.

recovery from the channel block is very slow, but can be enhanced by application of voltage ramp pulses as will be demonstrated later in this section (Fig. 4).

A noticeable block was already observed at a concentration of arachidonic acid [AA] = 1 μmol/l, and a complete block was observed at [AA] = 25 μmol/l. Higher concentrations ([AA] = 50 μmol/l) were definitely supramaximal.

Fig. 4 shows a complete block by 2.5 μmol/l of AA in a patch membrane with one activated maxi-Cl channel at the start of the experiment. The channel showed in Krebs solution several substates and flickerings as evident from the amplitude distribution between 0 and 10 pA. Soon after the introduction of AA containing Krebs solution (faded pink color) the unit activity disappeared. After 30 episodes

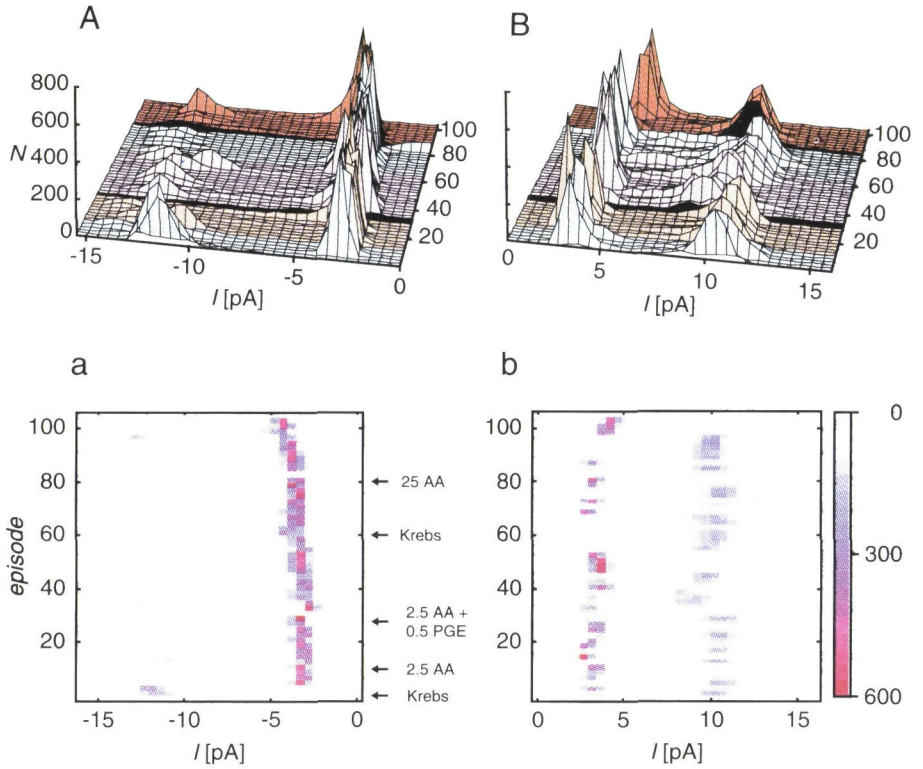

Figure 5. Three-dimensional graphs ($A - B$) and their two-dimensional projections ($a - b$) showing the absence of unit channel current modulation by arachidonic acid (2.5 and 25 μmol/l). One maxi-Cl channel in the patched membrane. Left (—) arrows denote introduction of specified solutions as discussed in the text. Ice blue color indicates records in Krebs solution, faded pink color indicates records in arachidonic acid (2.5 μmol/l) containing Krebs solution, hot pink color indicates records in 25 μmol/l arachidonic acid solution, magenta light color indicates records in 2.5 μmol/l arachidonic solution after addition of prostaglandin E1. The height of current peaks (N) in two-dimensional graphs is represented by different colors (see color scale).

the AA solution was exchanged for control Krebs solution (ice blue) with the result that only few substates recovered. The channel unit currents recovered, however, soon after application of a ramp pulse (from −40 to +40 mV) applied just before the exchange of solutions. The first response after the ramp pulse is shown in black. The supernormal recovery after the ramp pulse manifests itself by activation of the full amplitude second maxi-Cl channel, the presence of which was indicated at the start in Krebs solution by fibrillations as found in the eighth episode. These responses were inhibited after application of 25 μmol/l AA (hot pink color). The start of inhibition is characterized by decomposition of the Cl currents to several substates and flickerings (52nd episode).

We observed in some cases that the maxi-Cl channel was resistant to the arachidonic acid block (Fig. 5). Pannels *A*, *B*, *a*, *b* of this figure are constructed in the same way as those demonstrated in Figs. 2 or 4 except for the fact that the base line was not subtracted from the records; the closed state line is therefore shifted few pA towards negative (*A*) or (*B*) positive current values. Only one channel was present in the patched membrane in the demonstrated experiment. It is evident that there was no change in the current responses to ±20 mV pulses after application of 2.5 μmol/l arachidonic acid (10th episode) or 25 mmol/l AA (85th

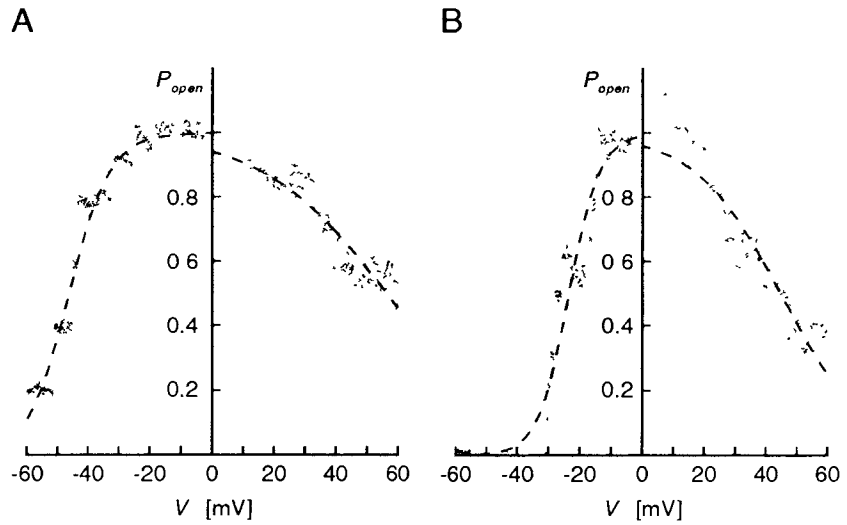

Figure 6. Voltage dependence (V) of the steady-state probability (P_{open}) of the channel being in the open state in control Krebs solution (*A*) and after application of arachidonic acid (2.5 μmol/l) (*B*), respectively. The same patch membrane as shown in Fig 5. The curve was fitted as the sum of two Boltzmann equations with the following coefficients; *A*: $V_h = -44.8$ mV and $k = -5.6$, respectively, for the negative side and +49.6 mV and +15.8 for the right side; *B*: $V_h = -22.6$ mV and $k = -4.9$, respectively, for the negative side and +42.1 mV and +12.9 for the right side.

episode), respectively. (The negative effect of 0.5 μmol/l prostaglandin E1, which was added (magenta light color) to the AA solution at about the 30th episode is not discussed in this paper).

One of the possibilities how to explain this observation, as well as the sudden recovery of the AA block by voltage ramps, is offered by the assumption that the arachidonic acid changes the voltage dependence (V) of the steady-state probability of the channel (P_0) being in the open state. Fig. 6 shows the voltage dependence of the probability (P_0) of the channel in the main open state, which was computed from 10 summated records of the channel activity to voltage ramp pulses from +10 to −60 mV and −10 to +60 mV, respectively, in Krebs solution (Fig. 6A) and in Krebs solution containing 2.5 mmol/l AA (Fig. 6B; measured at the end of the first AA trial shown in Fig. 5). Arachidonic acid shifted the midpoint potentials (Vh) to lower values both in the negative and positive range of potentials with a small decline in the slope factor (kn). The amplitudes of the pulses (±20 mV) are in the range of the bell-shaped relation, even if at the very border, which did not change in AA solutions. The block restoring effect of ramp pulses might be explained, if the effect of conditioning pulses, as described in the previous paper (Hurňák and Zachar 1994) is taken into account.

The blocking effect of stilbene derivatives (DIDS)

Fig. 7 shows the effect of stilbene derivative DIDS (4,4′-diisothiocyanato stilbene-2,2′-disulphonic acid) on the activity of the high-conductance Cl channel in bottom-attached L6 myoblasts. Panel A (first column) shows 4 out of 10 records of unit currents to repeated −30 mV voltage steps in control Krebs solution. The patch contained several (at least 4) maxi-Cl channels which inactivated fairly quickly at these membrane voltage steps, as evident from ensemble average membrane currents ($n = 10$) in the first column of panel B. The panel also shows the ensemble average currents to positive 30 mV voltage steps. After 2 min the flowing solution in the perfusion pipette enclosing the patch pipette was exchanged for Krebs solution containing 100 μmol/l DIDS. The sequence and duration of solution exchanges is demonstrated graphically in panel C. The records in the middle column of panels A and B were taken 5 min after introduction of the DIDS containing saline. There is a substantial reduction of ensemble average currents (B) to −30 mV voltage steps and practically almost complete disappearance of unit currents to +30 mV voltage displacement. The blocking effect of DIDS took place slowly with a time constant of 1–2 min as evident from the average amplitudes of the unit channel currents which were monitored continuously during the experiment by applying pulses of opposite polarity with 10 s interpulse interval. The recovery from 100 μmol/l DIDS was slow as demonstrated in right-hand columns in panels A and B, as well as by panel C. The continuous record in panel C shows also an interesting phenomenon which was repeatedly observed, i.e. a sudden recovery of the amplitudes of unit

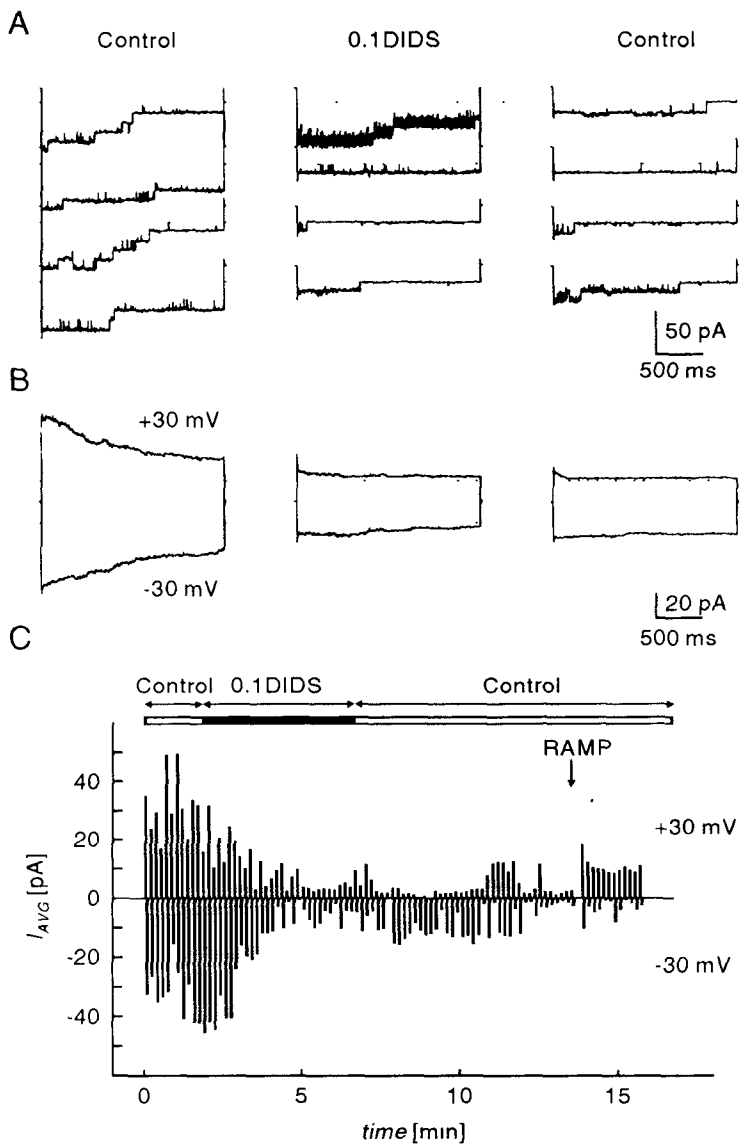

Figure 7. The effect od stilbene derivative DIDS (0.1 mmol/l) on single-channel currents recorded from an excised patch (inside-out) of an L6 myoblast in control Krebs solution, 5 min after addition of DIDS and 5 min after reintroduction of Krebs solution. *A*: Four consecutive single-channel current traces to repeated command potentials of −30 mV and 1998 ms in duration applied at 5 s intervals. The holding potential was 0 mV. *B*: Ensemble averages of single-channel currents to ± 30 mV pulses as partially shown in *A*. *C*: The bars represent average currents to successive positive and negative 30 mV pulses during the whole experiment to show the development and recovery from the DIDS block (see the inset diagram). The arrow indicates the application a ramp pulse.

currents after application of a voltage ramp pulse from −60 to +60 mV in 4s. The phenomenon could be related to a similar effect observed with the relieve of the arachidonic acid block and the effect of conditioning prepulses as described elsewhere (Hurňák and Zachar 1994).

A noticeable effect of DIDS was already observed at a concentration of 10 mmol/l and increased with increasing concentration of this silbene derivative; the concentration of 100 mmol/l seems to be maximal.

The blocking effect of Zn^{2+} ions

Fig. 8 demonstrates the blocking effect of Zn^{2+} ions (1 mmol/l) on single channel currents to repeated membrane potential displacements (−20 mV; 2 s in duration) from the holding potential of 0 mV in symmetrical physiological solutions. The time dependent inactivation of the channel activity at this membrane potential displacement was small and the channel remained in a state of a continuous activity showing frequent transitions from the open to closed state (*A*). Few minutes after addition of the Zn^{2+} ions (1 mmol/l) the channel fluctuations abruptly disappeared (the block ensued) without any previous change of the unit current amplitude (*B*). After reintroducing the control saline (physiological solution; see Materials and Methods) the channel activity reappeared (after about 5 min), but the amplitude of unit currents was smaller (*C*) than in controls before the start of the experiment. The full amplitude of single channel currents was recovered after few tens of min (*D*). It seems evident, upon inspection of the records during recovery, that the reduced current amplitudes can be rather ascribed to a lowered channel conductance than to an activity of the channel on a smaller subconductance level. The blocking effect of $ZnCl_2$ ions on single channel currents to positive 20 mV pulses (alternately applied with negative pulses) was similar (not shown); in spite of the fact that the single channel current rested more frequently in the open state.

Fig. 9 shows the effect of 5 mmol/l $ZnCl_2$ on the channel unit currents in an excised (inside-out) patch that contained three large-conductance chloride channels and was subjected alternately to voltage steps of ±40 mV from the holding potential of 0 mV. Fig. 9*A* shows five successive unit current records to voltage steps in hyperpolarizing direction before, during and after exposure to 5 mmol/l $ZnCl_2$ added to the basic saline. The corresponding ensemble average currents ob-

Figure 8. Four panels (*A* – *D*) of consecutive single-channel current traces (cut from long continuous recordings) to repeated command potentials of −20 mV and 2 s in duration applied at 10 s intervals. The holding potential was 0 mV. *A*: in control solution; *B*: 5 min after addition of Zn^{2+} ions (1 mmol/l); *C*: 4 min after withdrawal of Zn^{2+} ions. *D*: 15 min after withdrawal of Zn^{2+} ions.

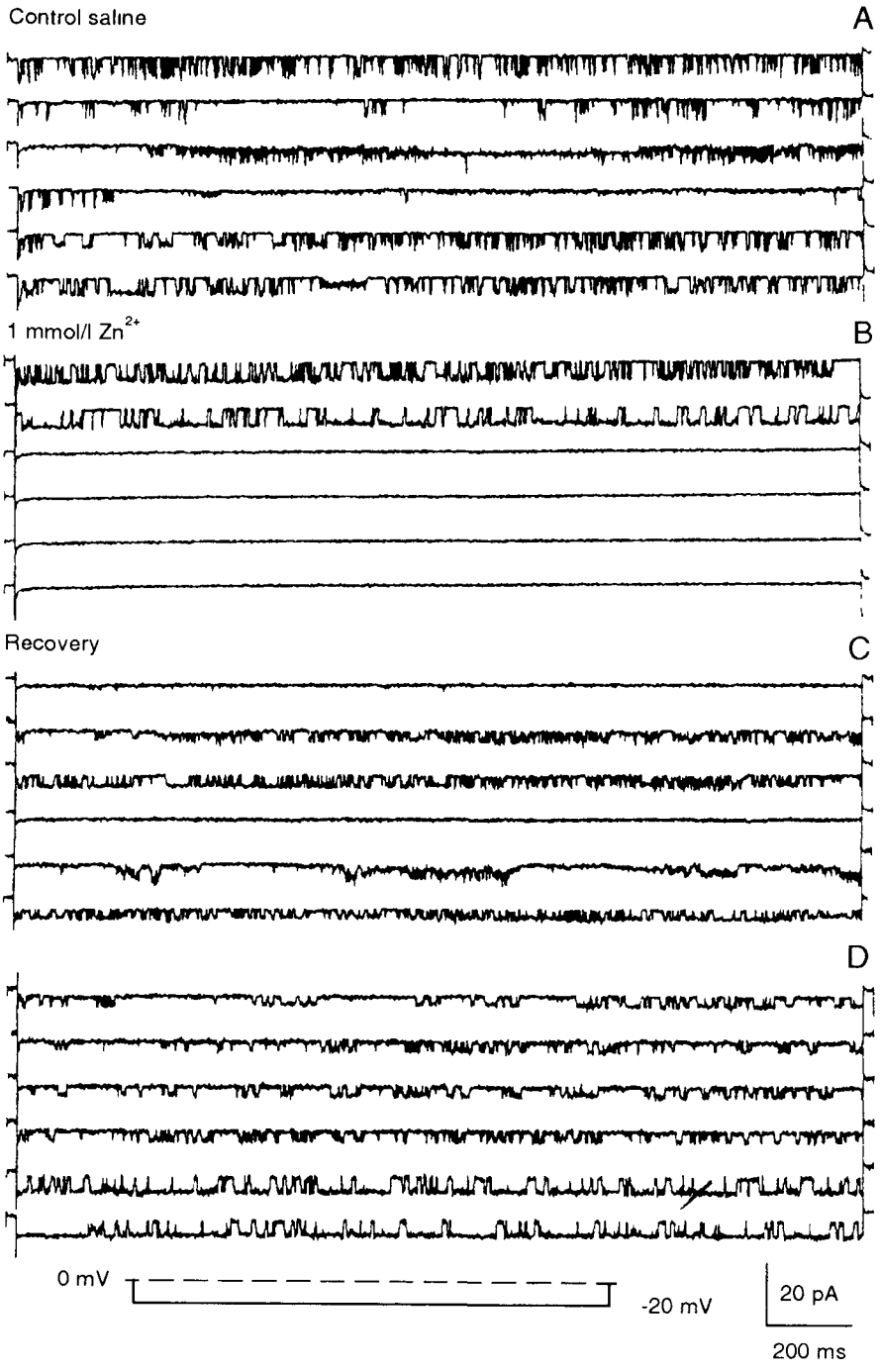
Control saline
A
1 mmol/l Zn^{2+}
B
Recovery
C
D
0 mV
-20 mV
20 pA
200 ms

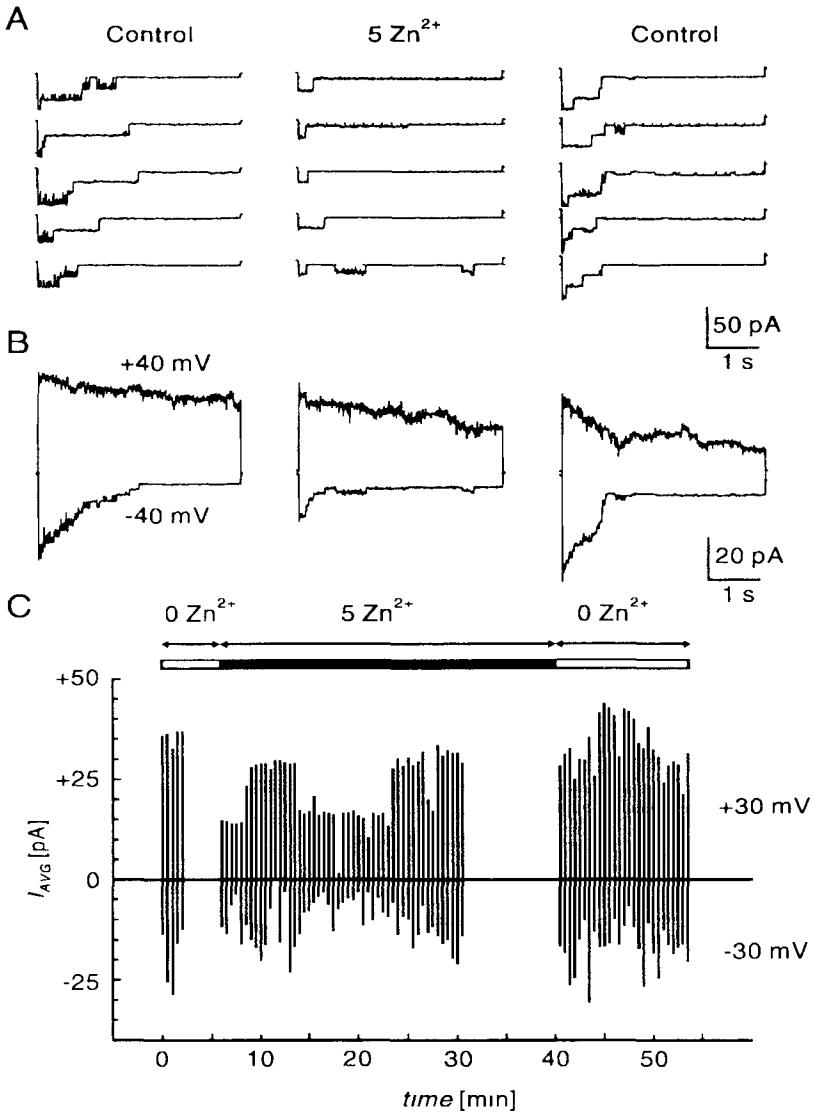

Figure 9. The effect of Zn^{2+} ions on the high-conductance chloride channel. The time course of the experiment is evident from the bottom panel. A Successive unit current records to −40 mV voltage steps. Duration of test pulses 1 s, interpulse interval 15 s, sampling interval 2 ms. Recordings in the left and the right panel are controls in symmetrical 150 mmol/l NaCl. The excised patch (inside-out) was then exposed to a test solution with $[Zn^{2+}] = 5$ mmol/l. Recordings in the middle were taken after 5 min in this solution. After 25 min the Zn^{2+} solution was exchanged for a control saline. The records in the right panel were energistered after 10 min in the recovery solution.

tained from 5 consecutive depolarizing and hyperpolarizing current responses are demonstrated in Fig. 9*B*. Three channels were activated in depolarizing direction, but only two in the hyperpolarizing direction. The most conspicuous change in responses to hyperpolarizing pulses was the inhibition of the second channel in the patch and prolongation of relaxation of the single channel activity, which remained active. The recovery from the blocking effect of Zn^{2+} was accompanied by facilitation as manifested by activation of the third channel in the patch membrane; the relaxation of the ensemble current was, however, accelerated. The blocking effect of $ZnCl_2$ ions is also evident on channel currents in the opposite direction, in spite of asymmetry of the response to negative and positive voltage steps. The number of responding channels was reduced and the time constant of relaxation was prolonged. During the recovery the relaxation of the ensemble average currents to positive voltage steps was accelerated.

Fig. 9*C* shows the average amplitudes of responses during single depolarization steps from 0 mV to ±30 mV in each condition; i.e. before, during and after the application of Zn^{2+} ions. The gaps in the record are due to cessation of recording to avoid the mains interference when preparing the exchange of solutions.

We did not find any significant change in the single-channel current amplitude in the presence of 5 mmol/l $ZnCl_2$ in this particular experiment, indicating that the inhibitory effect was due to reduction of the active channels in the patch membrane. The one channel containing patch (Fig. 8) is evidently more suitable for demonstration of the conductance change. Further increases in the concentration of $ZnCl_2$ to 10 mmol/l rendered Cl channels completely silent even in patches with multiple channels (not shown) and washing out Zn^{2+} then partially restored the activity of all channels. These results indicate that Zn ions reversibly block Cl channel from intracellular face.

Discussion

The effect of arachidonic acid

The direct blocking effect of arachidonic acid on large-conductance chloride channels represents a novel finding. Direct regulation of several types of ion channels by arachidonic acid and other fatty acids has been, however, demonstrated in a variety of cells (for review see Ordway et al. 1991). Direct effects are those which

Figure 9. (continuation) *B*. Ensemble average currents (5 records) to ±40 mV voltage pulses obtained in the absence and the presence of Zn^{2+} ions. The membrane patch contained 3 channels. *C*. Average amplitudes of the unit channel currents during a single depolarizing command pulse to +30 and −30 mV respectively in each condition (0 Zn^{2+}, 5 Zn^{2+}, 0 Zn^{2+}).

do not depend on the conversion of arachidonic acid to a variety of active oxygenated metabolites (Needleman et al. 1986), which then activate ionic channels. The patch-clamp technique allows to demonstrate the direct effects of arachidonic acid in a straightforward way, as the necessary machinery for conversion of the fatty acids in the lipoxygenase, cyclo-oxygenase or cytochrome P-450 pathway is absent in excised and superfused inside-out membrane patches.

The inhibitory effect of fatty acids on Cl^- channels at micromolar concentrations was first demonstrated in airway epithelia (Anderson and Welsh 1990; Hwang et al. 1990). The Cl^- current block by arachidonic acid was recently described also in intestinal epithelial cells (Kubo and Okada 1992). Sakai et al. (1992) found, on the contrary, activation of small-conductance Cl^- channels in parietal cells of gastric glands. These differences can be plausibly explained on the assumption that different types of Cl^- channels possess different epitopes for fatty acid interaction with the channel itself or an associated protein. There are at least four distinct kinds of Cl^- channels in epithelial cells (Franciolini and Nonner 1987; Hille 1992) which are to be considered in this connection: (a) the Cl^- channel with very small conductance (1–3 pS) (Evans and Marty 1986); (b) the small-conductance Cl^- channel (4–11 pS) activated by cyclic AMP (most probably identic with CFTR, cystic fibrosis transmembrane conductance regulator; Anderson et al. 1991); (c) the intermediate-conductance Cl^- channel (25–75 pS) (Li et al. 1988); (d) the large-conductance Cl^- channel (Krouse et al. 1986). The above mentioned inhibitory effects of fatty acids concern the outwardly rectifying, intermediate-conductance Cl^- channels. The activation of Cl^- channels (Sakai et al. 1992) by arachidonic acid concerns, on the other hand, the very small-conductance Cl^- channel and the effect is indirect as the activation was achieved by products of arachidonic acid metabolites as well.

The inhibitory effect of arachidonic acid on maxi-Cl channels in L6 myoblasts took place when the arachidonic acid was applied from the intracellular side of the membrane, and not from the extracellular side. This strict asymmetry of the effect was observed also in other preparations (Kim and Clampham 1989; Anderson and Welsh 1990), but a more common finding is represented by a modulatory effect from both sides of the channel, e.g. in excised inside-out and outside-out patch membranes containing K^+ channels (Ordway et al. 1989). Variation of the membrane target side of the arachidonic acid action might be possibly related to the role of this messenger system also in the intercellular communication (Mochizuki-Oda et al. 1993; Fraser et al. 1993).

The development of arachidonic acid block was characterized by changes in the dependence of the probability of the channel being in the open state on voltage. At submaximal concentrations the arachidonic acid shifted the midpoint potentials (V_h) to lower values both in the negative and positive range of potentials with the result that the currents to smaller displacements of membrane potential remained

intact, but those to larger membrane displacements were blocked. A similar kind of block of maxi-Cl channels was observed recently in inside-out patches from freshly isolated fetal type II alveolar epithelial cells after bath addition of GTPγS (100 μmol/l), a nonmetabolizable analog of GTP (Kemp et al. 1993). The midpoint potential of the negative branch of the Boltzman plot was shifted in these experiments about 20 mV closer to the holding potential similarly as in our experiments. It might turn out that both blocking agents have a common basis if it is assumed that the maxi-Cl channel in fetal alveolar cells is coupled to the G protein by means of fatty acid metabolism (Kurachi et al. 1989). It must be, however, explained why the large conductance anion channels in a renal epithelium are, on the contrary, activated by GTPγS (Schweibert et al. 1990).

The concentrations of the exogenously applied arachidonic acid that modulated the maxi-Cl channel in L6 myoblasts are in the same range as those used for the inhibition and/or activation of different kinds of channels (ranging from 1 to 100 μmol/l). These exogenous concentrations are similar to those that produce sufficient metabolites to emulate the activation of channels by agonists (Ordway et al. 1991). In proliferating cell culture conditions the endogenous arachidonic acid is most probably released from phospholipids in myoblast membranes by the action of phospholipases activated by agonist-stimulated membrane receptors or by some unknown intracellular factor related to the cell cycle metabolism. The arachidonic acid and fatty acids are in great abundance and strategically well located to be able to play a role of second messengers that regulate the maxi-Cl channels. The closure of the maxi-Cl channels by arachidonic acid, which is locally produced, might represent an efficient way to exclude the short-circuiting mechanism of the maxi-Cl channels on the resting membrane potential and thus modulate a number of cellular processes dependent on the membrane potential. Alterations of membrane potential (hyperpolarization) by arachidonic acid and other fatty acids were recently demonstrated using membrane-potential sensitive fluorescent dye in PC12 and bovine adrenal chromaffin cells (Ehrengruber et al. 1993).

The arachidonic acid block was compared with the effect of two groups of agents, which were shown to block the maxi-Cl channels in a number of cells, i.e. the stilbene derivatives and Zn^{2+} ions.

The effect of stilbene derivatives

The disulfonic stilbene derivatives, DIDS and SITS were widely used as blockators of large-conductance chloride channels since their first use for this purpose in A6 epithelial cells (Nelson et al. 1984). They are, however, non specific blockators as they block a number of chloride transporting systems as well, including other kinds of Cl^- channels (White and Miller 1979; Inoue 1985; Gray and Ritchie 1986; Gogelein 1988; Christensen et al. 1989) and anion exchangers (Rothstein et al. 1976; Knauf 1979). It is interesting to note in this connection that the maxi-Cl

channels can be blocked by furosemide assumed to block the Na^+/Cl^- cotransporter (Christensen et al. 1989). Block of maxi-Cl channels by stilbene derivatives varies to a great extent in different cell membranes. First of all, there are different sensitivities of the maxi-Cl channels to the intracellular and the extracellular application of the drug in different preparations. The absence of intracellular block of maxi-Cl channels by DIDS was demonstrated in adult skeletal muscle cells (with maximum blocking extracellular concentration of DIDS, $[DIDS]_e \approx 200$ μmol/l) (Woll et al. 1987) and the prevalence of extracellular block over the intracellular block was observed in T lymphocytes (Pahapill and Schlichter 1992), in endothelial cells (Groschner and Kukovetz 1992), and A6 epithelial cells (Nelson et al. 1984). A converse situation was reported to exist in A7r5 myoblasts (Kokubun et al. 1991) with $[DIDS]_e \approx 1$ mmol/l and $[DIDS]_i \approx 5$ μmol/l (the threshold intracellular concentration of DIDS), in a mouse B lymphocyte cell line (Bosma 1989), as well as in L6 myoblasts, as follows from our experiments described in this work. In spite of these differences the blocks of maxi-Cl channels by stilbene derivatives in different cells share a number of common properties. The block is usually characterized (e.g. Kokubun et al. 1991; Pahapill and Schlichter 1992) by the following properties: (1) reduction of open times and/or appearance of flickerings; (2) decrease in ensemble average currents; (3) disappearance of time dependent inactivation; (4) decrease in amplitude of single channel currents; (5) prevailing irreversibility of the block after wash out of the stilbene derivatives. With small aberrations these characteristics also apply to the block by DIDS in L6 myoblasts in our experiments. The flickering is clearly seen in Fig. 7A after application of DIDS (100 μmol/l); this panel also shows the decrease in amplitude of single channel current to a substate level. The decrease of ensemble average currents and the apparent loss of time dependent inactivation was shown in Fig. 7B. The block by DIDS in L6 myoblasts was clearly shown to be mostly irreversible. A new finding is, however, represented by a partial relief of the block by the interposed voltage ramp pulse. In this respect the DIDS block resembles that by arachidonic acid block as we described above. This partial reversibility could mean that the site of interaction of the stilbene derivative with the channel is different from that in the irreversible mode of blockade. If we follow the interpretation of Gray and Ritchie (1986) of a block in astroglial Cl^- channels, the irreversible component of the block could be ascribed to covalent binding of DIDS at a site that inhibits opening and the reversible component of the block to non covalent binding of DIDS to an open channel.

The blocking effect of Zn^{2+} ions

The blocking effect of Zn^{2+} ions on maxi-Cl channels was first described in amphibian skeletal muscle by Woll et al. (1987). The extracellular Zn^{2+} ions (0.1–1 mmol/l) blocked both the outward and inward single channel currents, whereas the intracellular Zn^{2+} ions (10 mmol/l) blocked only the outward currents, i.e.

the block was voltage-dependent when the ions were applied from the cytoplasmic side of the channel. The blocking effect of Zn^{2+} ions is not specific for maxi-Cl channels; the Zn^{2+} ions are known to block Na, K and Cl channels in frog skeletal muscle membrane (Hille et al. 1975; Stanfield 1970) at comparable concentrations. Similar voltage-dependent blocks after application of Zn^{2+} ions ($\geq$ 1 mmol/l) from the intracellular side of the channel were also demonstrated in maxi-Cl channels from vascular smooth muscle cells (Kokubun et al. 1991), from human T lymphocytes (Schlichter et al. 1990), and from pig aortic endothelial cells (Groschner and Kukovetz 1992). In the latter cells also a voltage independent zinc block was demonstrated upon application of Zn^{2+} ions (1 mmol/l) from the extracellular side. A voltage-independent block after application of Zn^{2+} ions (1 mmol/l) from the cytoplasmic side was reported in bleb-like vesicles from Schwann cells (Quasthoff et al. 1992). As we have shown, the Zn^{2+} ions (1 mmol/l) were equally effective both from the intracellular and extracellular side, respectively, also in L6 myoblasts. There is, however, a definite asymmetry in the blocking effect showing a preference for inward currents (Fig. 10). Therefore a kind of voltage-dependent block cannot be excluded. Reversibility represents a characteristic property of all zinc blocks so far examined in maxi-Cl channels. The same holds true for the large conductance Cl channels as evident e.g. from Fig. 8 or Fig. 9. The blocking effect is completely reversible as far as the peak amplitude is concerned, but the time dependent inactivation remained enhanced.

Acknowledgements. This work was supported partly by a grant (2/999039/93 GAV) to J. Z. The authors wish to thank Dr. Daria Zacharová for valuable suggestions during the course of experiments and useful comments to the manuscript.

References

Anderson M. P., Gregory R. J., Thompson S., Sousa D. W., Paul S., Mulligan R. C., Smith A. E., Welsh M. J. (1991): Demonstration that CFTR is a chloride channel by alteration of its anion selectivity. Science **253,** 202—205

Anderson M. P., Welsh M. J. (1990): Fatty acids inhibit apical membrane chloride channels in airway epithelia. Proc. Nat. Acad. Sci. USA **87,** 7334—7338

Axelrod J. (1990): Receptor-mediated activation of phospholipase A_2 and arachidonic acid release in signal transduction. Biochem. Soc. Trans. **18,** 503- 507

Bettendorff L., Kolb H.-A., Schoffeniels E. (1993): Thiamine triphosphate activates an anion channel of large unit conductance in neuroblastoma cells. J. Membrane Biol. **136,** 281—288

Bosma M. M. (1989): Anion channels with multiple conductance levels in a mouse B lymphocyte cell line. J. Physiol. (London) **410,** 67—90

Christensen O., Simon M., Randlev T. (1989): Anion channels in leaky epithelium. A patch-clamp study of choroid plexus. Pflügers Arch. **415,** 37—46

Ehrengruber M. U., Deranleau D. A., Kempf C., Zahler P., Lanzrein M. (1993): Arachidonic acid and other unsaturated fatty acids alter membrane potential in PC12 and bovine adrenal chromaffin cells. J. Neurochem. **60,** 282—288

Evans M G , Marty A (1986) Calcium-dependent chloride currents in isolated cells from rat lacrimal glands J Physiol (London) **378,** 437—460

Franciolini F , Nonner W (1987) Anion and cation permeability of a chloride channel in rat hippocampal neurons J Gen Physiol **90,** 453—478 (from Hille 1992)

Fraser D D , Hoehn K , Weiss S MacVicar B A (1993) Arachidonic acid inhibits sodium currents and synaptic transmission in cultured striatal neurons Neuron **11,** 633—634

Gogelein H (1988) Chloride channels in epithelia Biochim Biophys Acta **947,** 521—547

Gray P T A , Ritchie J M (1986) A voltage-gated chloride conductance in rat cultured astrocytes Proc Roy Soc London Ser B **228,** 267—288

Groschner K , Kukovetz W R (1992) Voltage-sensitive chloride channels of large conductance in the membrane of pig aortic endothelial cells Pflugers Arch **421,** 209—217

Hamill O , Marty A , Neher E , Sakmann B , Sigworth F J (1981) Improved patch-clamp techniques for high-resolution current recorded from cells and cell-free membrane patches Pflugers Arch **391,** 85—100

Hille B (1992) Ionic Channels of Excitable Membranes Second edition Sinauer Associates, Inc , Sunderland, Mass , USA

Hille B , Woodhall A M , Shapiro B I (1975) Negative surface charge near sodium channels of nerve Divalent ions, monovalent ions, and pH Phil Trans Roy Soc London Ser B **270,** 301—318

Hurňak O , Zachar J (1992) Maxi-chloride channels in L6 myoblasts Gen Physiol Biophys **11,** 389—400

Hurňak O , Zachar J (1993) High-conductance chloride channels in BC3H1 myoblasts Gen Physiol Biophys **12,** 171—182

Hurňak O , Zachar J (1994) Conductance-voltage relations in large-conductance chloride channels in proliferating L6 myoblasts Gen Physiol Biophys **13,** 171—192

Hwang T C , Guggino S E , Guggino W B (1990) Direct modulation of secretory chloride channels by arachidonic and other cis unsaturated fatty acids Proc Nat Acad Sci USA **87,** 5706—5709

Inoue I (1985) Voltage-dependent chloride-conductance of the squid axon membrane and its blockade by disulfonic stilbene derivatives J Gen Physiol **85,** 519—537

Irvine R F (1982) How is the level of free arachidonic acid controlled in mammalian cells? Biochem J **204,** 3—16

Kemp P J , MacGregor G G , Olver R E (1993) G protein-regulated large-conductance chloride channels in freshly isolated fetal type II alveolar epithelial cells Amer J Physiol **265,** L323—L329

Kim D , Clampham D E (1989) Potassium channels in cardiac cells activated by arachidonic acid and phospholipids Science **244,** 1174—1176

Knauf P A (1979) Erythrocyte anion exchange and the band-3 protein transport kinetics and molecular structure Curr Top Membr Transp **12,** 249 –363

Kokubun S Saigusa A Tamura T (1991) Blockade of Cl channels by organic and inorganic blockers in vascular smooth muscle cells Pflugers Arch **418,** 204—213

Krouse M E Schneider G T , Gage P W (1986) A large anion-selective channel has seven conductance levels Nature **319,** 58 60

Kubo M Okada Y (1992) Volume regulatory Cl channel currents in cultured human epithelial cells J Physiol (London) **456,** 351—371

Kurachi Y Ito H Sugimoto T Shimizu T Miki I Ui M (1989) Arachidonic acid metabolites as intracellular modulators of the G protein-gated cardiac K^+ C hannel

Nature **337,** 555—557

Li M., McCann J. D., Liedtke C. M., Nairn A. C., Greengard P., Welsh M. J. (1988): Cyclic AMP-dependent protein kinase opens chloride channels in normal but not cystic fibrosis airway epithelium. Nature **330,** 752—754

Mochizuki-Oda N., Negishi M., Mori K., Ito S. (1993): Arachidonic acid activates cation channels in bovine adrenal chromaffin cells. J. Neurochem. **61,** 1882—1890

Needleman P., Turk J., Jakschik B. A., Morrison A. R., Lefkowith J.B. (1986): Arachidonic acid metabolism. Annu. Rev. Biochem. **55,** 69—102

Nelson D. J., Tang J. M., Palmer L. G. (1984): Single-channel recordings of apical membrane chloride conductance in A6 epithelial cells. J. Membrane Biol. **80,** 81—89

Ordway R. W., Walsh J. W., Singer J. J. (1989): Arachidonic acid and other fatty acids directly activate potassium channels in smooth muscle cells. Science **244,** 1176—1179

Ordway R. W., Singer J. J., Walsh J. W. (1991): Direct regulation of ion channels by fatty acids. Trends Neurosci. **14,** 96—100

Pahapill P. A., Schlichter L. C. (1992): Cl-channels in intact human lymphocytes-T. J. Membrane Biol. **125,** 171—183

Piomelli D., Volterra A., Dale N., Siegelbaum S. A. (1987): Lipoxygenase metabolites of arachidonic acid as second messengers for presynaptic inhibition of *Aplysia* sensory cells. Nature **328,** 38—43

Quasthoff S., Strupp M., Grafe P. (1992): High conductance anion channel in Schwann cell vesicles from rat spinal roots. Glia **5,** 17—24

Rothstein A., Cabantchik Z. I., Knauf P. (1976): Mechanism of anion transport in red blood cells: Role of membrane proteins. Fed. Proc. **35,** 3—10

Sakai H., Okada Y., Morii M., Takeguchi N. (1992): Arachidonic acid and prostaglandin E2 activate small-conductance Cl^- channels in the basolateral membrane of rabbit parietal cells. J. Physiol. (London) **448,** 293—306

Schlichter L. C., Grygorczyk R., Pahapill P. A., Grygorczyk C. (1990):. A large multiple conductance Cl channel in normal human T lymphocytes. Pflügers Arch. **416,** 413—421

Schweibert E. M., Light D. B., Fejes-Toth G., Naray-Fejes-Toth A., Stanton B. A. (1990): A GTP-binding protein activates chloride channels in renal epithelium. J. Biol. Chem. **265,** 7725—7728

Stanfield P. R. (1970): The differential effects of tetraethylammonium and zinc ions on the resting conductance of frog skeletal muscle. J. Physiol. (Lond) **209,** 213—256

White M. M., Miller C. (1979): A voltage-gated anion channel from the electric organ of *Torpedo californica.* J. Biol. Chem. **254,** 10161—10166

Woll K. H., Leibowitz M. D., Neumcke B., Hille B. (1987): A high-conductance anion channel in adult amphibian skeletal muscle. Pflügers Arch. **410,** 632—640

Final version accepted May 10, 1994